

UNCLASSIFIED

DASA 2657

May 1971

AD 726746

STATIC UNIAXIAL DEFORMATION OF 15 ROCKS

FINAL REPORT

W.F. BRACE  
and  
D.K. RILEY

HEADQUARTERS

Defense Atomic Support Agency  
Washington, D.C. 20305

Department of Earth and Planetary Sciences  
Massachusetts Institute of Technology  
Cambridge, Massachusetts 02139

Contract No. DASA01-69-C-0122

DDC  
RECEIVED  
JUL 27 1971  
REGISTRY  
C

Approved for public release; distribution unlimited

Reproduced by  
NATIONAL TECHNICAL  
INFORMATION SERVICE  
Springfield, Va. 22151

UNCLASSIFIED

**BEST  
AVAILABLE COPY**

SECTION #		
DTI	WRITE SECTION	<input checked="" type="checkbox"/>
IS	DIFF SECTION	<input type="checkbox"/>
MANPOWERED		<input type="checkbox"/>
JUSTIFICATION		
BY		
DISTRIBUTION/AVAILABILITY CODES		
DIST.	AVAIL.	SPECIAL
A		

Reproduction of this document in whole or in part is prohibited except with permission of the Defense Atomic Support Agency. However, DDC is authorized to reproduce the documents for United States Government purposes.

Destroy this report when it is no longer needed.  
Do not return to sender.

## DOCUMENT CONTROL DATA - R &amp; D

(Security classification of title, body of abstract and indexing annotation must be entered when the overall report is classified)

1. ORIGINATING ACTIVITY (Corporate author) Massachusetts Institute of Technology Division of Sponsored Research		2a. REPORT SECURITY CLASSIFICATION UNCLASSIFIED	
		2b. GROUP	
3. REPORT TITLE "Static uniaxial deformation of 15 rocks"			
4. DESCRIPTIVE NOTES (Type of report and inclusive dates)			
5. AUTHOR(S) (First name, middle initial, last name) W.F. Brace and Don K. Riley			
6. REPORT DATE May 1971		7a. TOTAL NO. OF PAGES 56	7b. NO. OF REFS 38
8a. CONTRACT OR GRANT NO. DASA 01-69-C-0122		9a. ORIGINATOR'S REPORT NUMBER(S) DASA 2657	
8b. PROJECT NO. ARPA Order 862			
8c. Program Code 9F10		9b. OTHER REPORT NO(S) (Any other numbers that may be assigned this report)	
8d.			
10. DISTRIBUTION STATEMENT Approved for public release. Distribution unlimited.			
11. SUPPLEMENTARY NOTES		12. SPONSORING MILITARY ACTIVITY The Director Advanced Research Projects Agency Washington, D.C. 20301	
13. ABSTRACT Samples of 15 rocks with porosity ranging from nearly zero to 40 percent were deformed under the constraint of uniaxial strain by stresses which reached 30 kb. No faults formed, although widespread small scale fracturing accompanied the compaction of the more porous rocks. Rocks with porosity less than 2 percent recovered from a cycle of loading with negligible permanent strain. Calcite twinned extensively in Bedford limestone and white marble, and in the latter there was indirect evidence of recoverable flow. Rocks loaded uniaxially reached very nearly the same stress-strain state as rocks loaded first hydrostatically and, then, in triaxial compression. The onset of dilatancy for granite, limestone and marble was close to the stress in a triaxial experiment at which strain was uniaxial.			

14

KEY WORDS

LINK A

LINK B

LINK C

ROLE

WT

ROLE

WT

ROLE

WT

Uniaxial deformation, compaction,  
dilatancy, stress-strain path

May 1971

STATIC UNIAXIAL DEFORMATION OF 15 ROCKS

FINAL REPORT

(This work was supported by the Advanced  
Research Projects Agency under ARPA Order No. 862)

W.F. BRACE

HEADQUARTERS

Defense Atomic Support Agency

Washington, D.C. 20305

Department of Earth and Planetary Sciences

Massachusetts Institute of Technology

Cambridge, Massachusetts 02139

Contract No. DASA01-69-C-0122

Approved for public release; distribution unlimited

**BLANK PAGE**

## ABSTRACT

Samples of 15 rocks with porosity ranging from nearly zero to 40 percent were deformed under the constraint of uniaxial strain by stresses which reached 30 kb. No faults formed, although widespread small scale fracturing accompanied the compaction of the more porous rocks. Rocks with porosity less than 2 percent recovered from a cycle of loading with negligible permanent strain. Calcite twinned extensively in Bedford limestone and white marble, and in the latter there was indirect evidence of recoverable flow. Rocks loaded uniaxially reached very nearly the same stress-strain state as rocks loaded first hydrostatically and, then, in triaxial compression. The onset of dilatancy for granite, limestone and marble was close to the stress in a triaxial experiment at which strain was uniaxial.

## TABLE OF CONTENTS

INTRODUCTION .....	1
Previous work .....	2
The present investigation .....	4
THE ROCKS STUDIED .....	5
EXPERIMENTAL PROCEDURE .....	9
Jacket .....	9
Sample preparation .....	10
Strain measurement .....	11
Loading procedure .....	11
Compressibility .....	16
MICROSCOPIC OBSERVATIONS .....	17
Marble .....	17
Bedford limestone .....	18
Solenhofen limestone .....	19
Tuff, tonalite and sandstones .....	19
DISCUSSION .....	19
Reproducibility .....	19
Recoverable behavior .....	20
Permanent strain .....	23
Path dependence of the stress-strain relation .....	24
Dilation and failure in relation to uniaxial deformation .....	27
Implications for failure theory of rocks .....	30

TABLE OF CONTENTS (continued)

ACKNOWLEDGMENTS .....	31
REFERENCES .....	32
FIGURE CAPTIONS .....	37

LIST OF TABLES

1. Rocks studied .....	6
2. Stresses, strains and porosity change during uniaxial strain loading .....	12

LIST OF FIGURES

1. Stress-strain relations during uniaxial loading ...	39
2. Stress in the axial direction as a function of axial strain .....	40
3. Photomicrographs of Bedford limestone (a) before deformation and (b) after one cycle of loading .	41
4. Uniaxial strain behavior of Westerly granite .....	42
5. Comparison of permanent volumetric compaction with initial porosity .....	43
6. Comparison of axial strains in uniaxial loading (a) and in hydrostatic plus triaxial loading (b).	44
7. Dilation stress and uniaxial deformation compared for Westerly granite .....	45
8. Dilation stress and uniaxial deformation compared for marble .....	46
9. Path dependence of uniaxial deformation for Solenhofen limestone .....	47
10. Stress at fracture and dilation compared for Westerly and Kitashirakawa granites .....	48

## INTRODUCTION

In a state of uniaxial strain, two of the principal strains are zero. Strain is usually assumed to be uniaxial in material loaded by a plane shock wave; this type of loading is achieved in impact experiments [ 1 ], and approximately in underground nuclear explosions [ 2 ]. The unique strain direction is perpendicular to the shock front. In tectonically inactive regions of the Earth's crust where, for example, vertical compaction in flat-lying rocks is taking place, strain may also be uniaxial [ 3 ].

The mechanical behavior of rock loaded in uniaxial strain is poorly understood. Few experimental studies are available. How, for example, do rocks fail in uniaxial strain, and is behavior prior to failure in any sense predictable from independent measurement of elastic properties? What is the role of porosity? One might suspect that rocks of high porosity will respond to this type of loading quite differently from those of low porosity. Finally, what is the role of strain rate? Do rocks deformed in uniaxial strain behave the same at high strain rates (shock loading) as at low strain rates (geologic loading)? The present study was designed to throw light on questions such as these. In addition, experiments in uniaxial strain provide a means of exploring path dependence of the stress-strain relation for rocks. This too is a subject which has received scant attention in rock mechanics.

## Previous work

SERATA [ 4 ] investigated rock-salt, limestone, and dolomite under conditions approximating uniaxial strain. Cylindrical samples were compressed axially while being restrained laterally by thick-walled steel cylinders. The lateral strains were not zero in his experiments, but were quite small. SERATA reported yielding in his materials, particularly in the rock-salt. Unfortunately, the materials he used have little application to the problem at hand, and there is some question as to the exact conditions of strain in his experiments. HENDRON [ 5 ] and TZUNG [ 6 ] tested a variety of sands at quite low pressures using a triaxial configuration in which lateral deformation of material was monitored. Confining pressure was varied so as to maintain zero lateral strain. BROWN et al [ 7 ] and SMITH et al [ 8 ] studied the behavior of several rocks (granite, tuff, diabase, rhyolite, and concrete) in uniaxial strain, using HENDRON's technique. They were capable of applying axial stress to 5 kb and confining pressure to 2 kb. The sample used was a very short cylinder. They reported a number of interesting characteristics of the elastic behavior of their materials, including maxima in the moduli at around a kilobar stress. No failure of their rocks was reported. The significance of porosity was not particularly clear, although they observed some densification of their more porous materials. BROWN and SWANSON [ 9 ] loaded Westerly granite, Cedar City tonalite and a quartzitic sandstone

(the Nugget sandstone of this study) in uniaxial strain as well as along other loading paths. Their main object was development of constitutive relations for rocks, although they investigated several of the questions posed above. They reported, for example, that volume contraction during uniaxial strain of Westerly granite was closely predictable from compressibility. They found no evidence of failure in the granite for stress as high as 11 kb. Their technique of loading and strain measurement was nearly identical to that used here, although they were limited to confining pressure of about 6 kb. Loading rate was similar to this study. No microscopic observations were given.

A number of rocks have been subjected to shock loading in order to determine an equation of state (see, for example, MCQUEEN et al [10]; LOMBARD [11]; AHRENS and GREGSON [12]) or fracture or yield characteristics (for example, PETERSEN et al [13]; AHRENS and ROSENBERG [14]; GIARDINI et al [15]). There have been few attempts to correlate shock results with laboratory experiments; strain rates in the former reach  $10^7 \text{sec}^{-1}$ , in the latter, range from  $10^{-3}$  to  $10^{-6} \text{sec}^{-1}$ . One noteworthy study is that of FROULA and JONES [1] who studied Westerly granite, Solenhofen limestone, Cedar City tonalite, and Nevada Test Site tuff. Solenhofen limestone behaved linearly up to crushing at a stress of 6 kb; the crushing observed at higher stress was time-dependent. Westerly granite behaved elastically to the maximum stress of 45 kb applied during their experiment. Based on a reinterpretation of the granite data, GREGSON, ISBELL, and

GREEN [16] reported evidence of yield in the granite at a stress of about 17 kb.

### The present investigation

In this paper attention is focussed in experimental procedures used in uniaxial strain loading, and on both macroscopic and microscopic aspects of the deformation. In companion papers a comparison of shock and static deformation of three of the rocks is given [17], and the recoverable, quasi-elastic behavior of certain of the rocks is analyzed [18].

Our experimental procedure followed closely that of BROWN et al [7] and BROWN and SWANSON [9], who used jacketed cylindrical samples of rock with strain gauges fixed to the surface to measure axial ( $\epsilon_1$ ) and circumferential ( $\epsilon_3$ ) strains. Pressure and axial stress were applied to the sample and varied independently in such a way that the lateral strain  $\epsilon_3$  was maintained equal to zero. The two stresses,  $\sigma_1$  and  $\sigma_3$ , were observed during loading as well as the single strain  $\epsilon_1$ , which equals volume change. Compression here is a positive stress; volumetric compaction is a positive strain.

A suite of rocks from our previous studies was particularly chosen for the problems at hand. Porosity ranged from 40 percent to nearly zero; composition covered typical igneous rocks, schist, tuff, and sandstone. As many rocks as possible were included from previous shock studies for our comparison of shock and static behavior [17].

We report here the stress-strain relations for these materials under uniaxial loading to stresses which reached about 30 kb, a limit set by our ability to generate a confining pressure and, therefore, a lateral stress of 10 kb. For approximately half the suite of rocks, strains were nearly recoverable in our experiments, and for these compressibility was determined to 10 kb. This served two purposes; it provided a sensitive test of cracking by comparison of initial compressibility before and after loading, and it enabled us to compare volumetric strains in uniaxial and hydrostatic situations, as in the work of BROWN and SWANSON [9]. Also for these rocks, static Poisson's ratio was measured as a function of pressure. This provided a comparison with the value obtained from the relation between  $\sigma_1$  and  $\sigma_3$  during uniaxial loading [18].

#### THE ROCKS STUDIED

Bulk density, total porosity, and modal analysis of the rocks studied are listed in Table 1. As indicated, most of the rocks have been investigated before in our studies of elastic and electrical properties. The Cedar City tonalite was supplied by S. Blouin of Kirtland Air Force Base. It is from the same general area as material studied in [1], [22], and [9]. A detailed petrographic description is given in [22].

TABLE 1. Rocks studied

6

Rock	Porosity %	Modal analysis	Density g/cm <sup>3</sup>	Reference
Diabase, II Frederick, Md.	0.1	49 an <sub>45</sub> , 46 pyr, 3 ox, 2 mica	3.03	19
Gabbro San Marcos, Cal.	0.2	70 an <sub>42</sub> , 12 mica, 8 pyr, 7 am, 3 ox	2.82	19
Schist source unknown	0.3	40 qu, 26 mica, 15 or, 7 an <sub>5</sub> , 7 gar, 5 ox	2.79	--
White marble source unknown	0.3	99 ca	2.70	19
Lynr felsite Saugus, Mass.	0.3	40 or, 35 an <sub>30</sub> , 25 qu, 2 ox, 1 mica	2.66	19
Limestone II Oak Hall, Pa.	0.6	98 ca-do, 1 qu, 1 ox	2.74	19
Granite Barre, Vt.	0.6	26 qu, 25 or, 37 an <sub>10</sub> , 12 mica	2.64	20

Granite	0.9	27.5 qu, 35.4 mi, 31.4 an <sub>17</sub> ,	2.62	21
Westerly, R. I.		4.9 mica		
Nugget sandstone	1.9	99 qu	2.54	9
Utah				
Pottsville sandstone	2.9	46 qu, 41 or, 11 mica, 2 ox	2.55	19
Tennessee				
Limestone	4.8	99 ca	2.54	21
Solenhofen				
Tonalite	7	55 an <sub>20-50</sub> , 20 qu, 8 pyr, 5 mica,	2.48	23
Cedar City, Utah		2 ox		
Limestone	12	99 ca	2.34	19
Bedford, Ind.				
Navajo sandstone	15.5	99 qu, 1 ox	2.24	--
source unknown				
Rhyolite Tuff	40	33 gl, 20 qu, 40 or, 4 an <sub>10</sub> , 2 ox	1.75	19
Colorado				

TABLE 1 (con't)

ABBREVIATIONS

qu	quartz	mica	mica clay
or	orthoclase	gl	glass
ca	calcite	gar	garnet
do	dolomite	ox	oxides
pyr	pyroxene	mi	microcline
	an	plagioclase	

Our specimens of Westerly granite and Solenhofen limestone are from different blocks as those of [9] and [1]. The Navajo sandstone is from an unknown location. The Nugget sandstone (quartzitic sandstone of [9]) comes from Parleys Canyon, Salt Lake County, Utah. The schist was supplied by Dr. Larry Schindler, OCE, from an undisclosed site. The Barre granite is from material currently being quarried at Barre, Vermont. Porosity was determined by immersion [21], and for the new materials here has an uncertainty of 0.002.

## EXPERIMENTAL PROCEDURE

### Jacket

The function of the jacket was twofold, to exclude the hydrostatic pressure medium from the rock sample, and to provide a smooth continuous surface for mounting strain gauges. Inasmuch as circumferential strains were to be maintained equal to zero during the experiments, circumferential strain in the jacket would also be negligible, so that radial constraint due to the jacket did not have to be considered. Seamless tubing 1.85 cm ID and 0.033 cm wall thickness of annealed copper was used; spun caps of copper were soft soldered to the tubing.

## Sample preparation

Precisely ground right circular cylinders, 1.85 cm in diameter and 3.8 cm long, were prepared from rock cores. At this stage porosity was determined. Then, the rocks of low porosity were jacketed as described above. The porous materials (porosity greater than a few percent) were given special treatment prior to jacketing.

Previous work had shown that porous rocks such as the tonalite or the Indiana limestone cannot be jacketed and gauged in the usual manner. Under high pressure the jacket is forced into surface pores; failure of the jacket often occurs. Even without failure, the apparent strain reported by the gauges is often very different from the true strain in the interior of the rock. To prevent collapse of jacket and gauges into surface pores, a filled epoxy was applied to the surface of the rock prior to jacketing. The filler was metal powder so chosen that the elastic properties of the cured epoxy approached that of the minerals. In a previous study of the tonalite [24], this procedure prevented surface pore collapse under pressure; strains recorded from measurements at the curved surface of samples treated in this manner agreed with those measured externally.

Before strain gauges were mounted, the jacketed samples were subjected to several hundred bars confining pressure. This seated the jackets firmly against the surface of the samples and also revealed jacket leaks. If dimples and other

depressions appeared at this stage in the jacketed surface, they were filled with solder and smoothed with a hand grinder.

### Strain measurement

Strain gauges were BLH epoxy-backed foil types (FAE-50-12S6 or FAE-100-12S6) cemented with EPY-150 cement cured according to manufacturers specification, using the additional precautions outlined in [25]. They were mounted axially and circumferentially on the samples.

The effect of pressure on strain gauges was taken into account following [26]. The pressure effect for the present gauges was  $+0.60 \times 10^{-7} \text{bar}^{-1}$ . The apparent strain in the axial direction,  $\epsilon_1$ , was corrected for the pressure effect in the usual way; the corrected quantity is given in Table 2.

The circumferential strain was to be maintained equal to zero. Because of the pressure effect on the gauge, this required that the gauge indicate an apparent strain exactly equal to the pressure effect. The experiments were so conducted that this condition was satisfied.

### Loading procedure

The gauged samples were pressurized (medium was petroleum ether) and loaded in a large screwdriven press. Pressure was generated externally, and recorded together with total axial force exerted by the press and the two strains as described above. Procedure was somewhat different for low and



Oak Hall Limestone

σ <sub>1</sub>	1.35	2.63	4.74	6.69	8.40	10.0	11.3	12.4	13.8	14.9	16.0
ε <sub>1</sub>	14.5	26.6	48.7	70.0	89.2	107	122	136	150	164	177
η <sub>p</sub>	←-50										

Barre Granite

σ <sub>1</sub>	2.19	3.71	5.96	8.55	10.8	12.9	14.9	16.8	18.7	20.5	22.3
ε <sub>1</sub>	32.4	49.6	82.4	111	138	165	189	212	236	257	277
η <sub>p</sub>	~3										

Westerly Granite

σ <sub>1</sub>	1.96	3.37	5.77	8.50	10.9	13.2	15.5	17.6	19.8	22.0	24.1
	--	3.16	6.00	8.51	11.0	13.2	15.4	17.6	19.7	21.7	--
ε <sub>1</sub>	26.6	45.2	76.2	107	136	165	192	219	246	271	298
	--	42.8	77.9	110	141	171	198	226	253	279	306

η<sub>p</sub>  
-3.0  
-4.2

Nugget Sandstone

σ <sub>1</sub>	3.14	4.86	8.40	11.6	14.4	17.3	20.1	22.6	24.9	26.8	28.5
ε <sub>1</sub>	62.0	103	168	225	276	325	371	412	450	483	516
η <sub>p</sub>	>0.5										

Pottsville Sandstone

σ <sub>1</sub>	2.56	4.72	8.67	12.1	15.6	18.4	21.2	23.9	26.1	28.6	30.9
ε <sub>1</sub>	61.0	100	175	237	301	343	393	439	471	523	566
η <sub>p</sub>	~+260										

TABLE 2 (Cont.)

Solenhofen Limestone											
1.28	2.32	4.54	5.84	6.89	7.82	8.71	9.68	10.7	11.7	12.7	
13.3	28.2	56.5	84.8	118	158	217	267	323	388	457	
+230											
Tonalite											
2.26	3.71	6.30	8.60	10.7	12.9	14.8	16.8	18.7	20.5	22.4	
107	171	251	324	386	440	493	541	587	627	668	
+420											
Bedford Limestone											
1.45	2.02	3.32	4.69	6.00	7.27	8.57	9.71	11.0	12.1	13.4	
93.0	175	448	675	855	979	1070	1170	1250	1310	1360	
+900											
Navajo Sandstone											
1.80	3.22	5.26	6.75	8.34	10.1	11.7	13.5	15.2	17.0	19.0	
62	134	285	454	590	725	850	955	1050	1140	1210	
+910											
Rhyolite Tuff											
1.58	2.39	3.79	5.54	7.35	9.23	11.2	13.0	14.8	16.6	18.3	
115	217	546	746	940	1170	1360	1480	1530	1650	1760	
+1310											

high porosity rocks. For the latter, application of pressure or axial compression generally caused permanent compressive strain, whereas for the former, strains were typically recoverable. For the low porosity rocks only, compressibility was determined before and after uniaxial strain loading. As noted above, the purpose was to detect possible cracking during uniaxial strain loading. A pressure of about 1 kb was applied for two or three cycles.

During an actual experiment, procedure was as follows. The sample was placed inside the pressure vessel and leads were connected to the strain gauges. The motor driven screw was then advanced at a rate equivalent to a strain of about  $10^{-5}\text{sec}^{-1}$ . A continuous record to axial force vs confining pressure was made, as well as a record of pressure vs both strains. As soon as the axial piston contacted the sample, load began to increase; pressure was then manually raised so as to maintain the circumferential strain equal to zero. As the piston advanced, continuous plots were made until the fluid pressure reached 10 kb, which was the limit of our pumping system. Axial load and then pressure were dropped, and in the case of the low porosity samples, compressibility to 1 kb re-measured. For the high porosity rocks, final external dimensions were measured with a micrometer.

Axial load was measured with an external force cell which had been calibrated against a proving ring. Accuracy

of force measurement was about 1 percent. A correction for O-ring friction at the pressure vessel seals was applied to the measured force during data reduction.

Pressure was measured by a manganin coil which also, through a bridge, provided an electrical signal suitable for recording. Accuracy was about 0.5 percent.

Strains were accurate to no better than 1 percent of the measured value, the uncertainty in the gauge factor. The condition of no circumferential strain could be maintained to about  $\pm 25 \times 10^{-6}$ . It is not known how strain gauge characteristics change for strains as large as those recorded for the more porous samples (up to 17 percent). Considerable uncertainty, perhaps as high as 10 percent, must be attached to the values of  $\epsilon_1$  given below which exceed a few percent.

The data are collected in Table 2 and plotted in Figs. 1 and 2 for the fifteen rocks. Duplicate samples of Westerly granite were run to test reproducibility so that two sets of data appear for that entry in Table 2.

### Compressibility

Measurement of linear strain as a function of hydrostatic pressure was carried out for the low porosity rocks for two reasons. First, increase in crack porosity during uniaxial strain loading could be estimated using the procedure outlined in [25]. Second, change in volume as a function of pressure could be compared with volume changes during uniaxial

loading [18]. In Table 2 the nonrecoverable strain, or new crack porosity, remaining after one cycle of uniaxial strain loading is given as  $\eta_p$ . This is given for the calcite rocks (marble and limestones) even though it was likely that plastic flow has occurred; this is known [27] to cause anomalous length changes upon release of pressure that may have nothing to do with cracks.

### MICROSCOPIC OBSERVATIONS

The rocks in Table 2 are listed in order of increasing initial porosity. This is also very nearly in order of increasing compaction as given by  $\eta_p$ . Homogeneous compaction in the axial direction was in fact the only obvious mode of deformation. The samples contained no faults, or fractures larger than the grain size. All of the rocks below the Nugget sandstone in Table 2 were sectioned to obtain further details of the deformation. A section of the marble was also prepared when we observed [18] that the effective Poisson's ratio of this rock had reached a value close to 0.50.

#### Marble

A thin section of the marble cut parallel with the sample axis revealed extensive twinning compared with untested material. Traces of the twins were typically 10 to 45° to the axis, and therefore to the  $\sigma_1$  axis. Twin spacing was compared in tested

and untested marble. The average for 50 grains in untested was 3.6 twins/mm compared with 11.4 twins/mm for the tested sample, as measured on the flat stage. Twins in more than one direction in a single grain were common in tested material.

### Bedford limestone

Our measurements, Table 2, revealed that much of the original porosity of the Bedford limestone had been eliminated during uniaxial deformation. This was borne out by study of the thin sections, which also revealed interesting details of the mechanics of compaction. Elimination of porosity is clearly seen in the pair of photomicrographs (Fig. 3) made of untested and tested material. Considerable plastic deformation of the individual grains is evident in the deformed sample. Twinning is quite abundant in the calcite which formed the cement between the shell fragments and other debris in the original rock. Some of the fossil fragments, nearly circular in cross section originally, became elliptical during uniaxial strain deformation. Measurement of axial lengths as seen in thin section show that apparent strains in the  $\sigma_1$  direction ranged from 5 to 15 percent; owing to original ellipticity of the fossil fragments, actual strains were probably closer to the smaller value. This number may be compared with the  $\epsilon_1$  of 9.8 percent (Table 2) caused by uniaxial deformation.

### Solenhofen limestone

An especially thin section was prepared of this fine-grained rock to see if plastic deformation of calcite had occurred here too. No twins were observed, although the 20 micron grains could be clearly resolved.

### Tuff, tonalite and sandstones

All of these rocks became less porous (Table 2) by amounts which ranged up to 13 percent of total volume. In thin section the deformed material appeared minutely fractured, but unfortunately in a way which could not be easily distinguished from untested material. Perhaps the difficulty lay with thin section preparation, which, particularly in the case of the tonalite, may have introduced microfractures about the same size as those produced during deformation. In any event, details of the compaction mechanism in these rocks were not obvious in thin section. Clearly, there is need for further work in this area.

## DISCUSSION

### Reproducibility

Results for Westerly granite are plotted in Fig. 4 as  $\sigma_1$  vs  $\sigma_3$  and  $\sigma_1$  vs  $\epsilon_1$ . The two samples studied here were virtually identical in the  $\sigma_1$ - $\sigma_3$  plot (see also Table 2) and

very close to that of [9], whose values are also shown in Fig. 4. In the  $\sigma_1$ - $\epsilon_1$  plot, our two samples differed by about two percent and were within a few percent of the BROWN and SWANSON values. Data from two different shock experiments are also given in Fig. 4 for comparison with our static values. The differences, which are seen to be small, are discussed in [17]. One of the shock studies was done on the so-called Bradford granite [28], which is said to come from a quarry adjacent to that of Westerly granite.

Agreement in  $\sigma_1$ - $\sigma_3$  for granite is probably as good as can be expected for two different laboratories, particularly when the samples are not taken from the same block of rock. The agreement in the  $\sigma_1$ - $\epsilon_1$  for Westerly is also quite satisfactory.

#### Recoverable behavior

Recovery as opposed to yield is defined in terms of  $\eta_p$ . A sample is said to recover if, after a cycle of uniaxial strain loading,  $\eta_p$  had a magnitude less than  $0.5 \times 10^{-4}$ . Much smaller strains than this can be detected when strain gauges are used in more conventional applications, but in view of the large strains imposed here this is quite a satisfactory limit.

$\eta_p$  (Table 2) is small and typically negative (denoting a permanent increase in volume) for all the rocks through

Nugget sandstone; for the more porous rocks making up the balance of the Table,  $\eta_p$  ranges up to 13.1 percent. Behavior of the first group, which recovered, is discussed in [18]; that of the second, in which permanent volumetric compaction took place, is considered in the next section.

The small extensions shown by many of the rocks may be a manifestation of the effect first noted by PATERSON [27] and more recently studied in detail by EDMOND [29]. For a wide variety of ductile rocks (limestone, marble, soapstone, polycrystalline alkali halides, and talc, and serpentinites) they observed a permanent increase in volume during the release of pressure following triaxial deformation to large permanent axial strains. The volume increase was particularly marked for the calcite rocks. It is of interest that in our study marble and Oak Hall limestone increased in volume 50 to 60 x 10<sup>-4</sup>. This might imply, according to [27], that some plastic deformation of these materials took place during uniaxial strain. As we noted above, this was substantiated by our microscopic study of the marble. A small increase in volume for schist, felsite and both granites was also noted (Table 2), although plastic flow of these materials in our experiments seems unlikely.

The volumetric strain,  $\epsilon_1$ , for all the rocks are compared as a function of  $\sigma_1$  in Fig. 2. The curves for the rocks which recovered are seen to be very nearly linear, whereas, with the

exception of Pottsville and Nugget sandstones, all of the others are strongly curved. The marked linearity and small permanent strains of the low porosity rocks suggests that the recoverable behavior was largely elastic. Elsewhere we analyzed this behavior [18] and found that volumetric compression during uniaxial strain was closely predictable from independent measurements of compressibility for diabase, gabbro, schist, marble, and two granites. However, the Poisson's ratio in uniaxial strain was appreciably higher than given by direct measurement. The difference could be explained by sliding motion on closed cracks, combined, in the case of marble, with flow of calcite.

Behavior of the marble in uniaxial strain was unusually interesting, as it may be an example of recoverable plastic flow. As noted in Table 2, recovery from the strain of about 2 percent was nearly complete, although there seemed compelling microscopic evidence of flow in the calcite grains, and the apparent Poisson's ratio during uniaxial deformation was nearly 0.50 [18]. The question immediately arises, did some of the calcite untwin during unloading, or did one set of grains twin during loading and another, differently oriented set twin during unloading? This question could probably be resolved by careful petrofabric analysis, which was, unfortunately, beyond the scope of the present study.

## Permanent strain

Appreciable permanent or nonrecoverable strain,  $\eta_p$ , was observed for all of the rocks having porosity greater than about 2 percent. This took the form of an apparently homogeneous one-dimensional compaction. As noted above, no faults, fractures or offsets larger than the grain diameter were observed.

The magnitude of the permanent strain,  $\eta_p$ , correlates fairly well with initial porosity (Fig. 5). The 45° line in this figure represents the maximum value of  $\eta_p$ . Pottsville sandstone and Bedford limestone are apparently quite close to this limit; the others are within about 40 percent of complete compaction. It is interesting that the degree of compaction does not always improve with the rocks which have the lowest strength, as might be expected. (Compare the stronger tonalite and weaker rhyolite, for example.) Probably a great many factors affect the degree of compaction at any given pressure, including grain size, shape of the pores, mineralogy, degree of alteration, and abundance and continuity of cracks.

In Fig. 2, the shapes of the  $\sigma_1$ - $\epsilon_1$  curves for the high porosity rocks may be compared. The curves are of two types, those initially concave upward (Pottsville sandstone and tonalite) and those initially concave downward. This difference is probably due to differences in crack porosity; from electrical studies [19], rhyolite, Bedford limestone and Solenhofen limestones are known to have little or no crack porosity, whereas Pottsville sandstone does.

The stress at which total compaction might occur can be roughly estimated from Fig. 2. The dotted lines give curves which would be followed for the different rocks if porosity were zero. They are obtained from the known elastic properties of rocks of the same composition; they intersect the abscissa at  $\epsilon_1$  equal the porosity. For example, the dotted line for Solenhofen limestone has about the same slope as the solid line for marble; it intersects the strain axis at 4.8 percent, the value of the porosity of the limestone. The stress at which the measured curves intersect these dotted lines would be the stress at which porosity reaches zero. For the two limestones, this stress appears to be 15 to 20 kb. For the Navajo sandstone this stress probably exceeds 30 kb. For the tonalite it may be a great deal higher.

From the shape of the curves in Fig. 3, the stress at which pore closure began for tonalite, rhyolite and Bedford limestone was apparently very low; data were not recorded at very low stresses, so that the actual magnitude cannot be definitely established. Finally, it is also of interest that for the two high porosity limestones, the stress at which pore collapse began seems to correlate inversely with the initial porosity (compare Figs. 2 and 5), as might be anticipated.

#### Path dependence of the stress-strain relation

The uniaxial strain experiments provide an opportunity to test the dependence of stress-strain behavior of certain of the

rocks upon loading path. This interesting theoretical question has, to our knowledge, only been considered previously by BROWN and SWANSON [9]. They found that stresses at faulting in Westerly granite and the tonalite did not differ by more than 5 or 10 percent for several stress paths. Here, we do not compare stresses at faulting but rather the stresses and strains when strain is uniaxial. This is done two ways. Referring to Fig. 6, we first compare the strains in the  $\sigma_1$  direction when strain in the  $\sigma_3$  direction is zero. In Fig. 6a the strain,  $\epsilon_U$ , is just the value found above during uniaxial strain loading and referred to in Table 2 as  $\epsilon_1$ . We compare  $\epsilon_U$  with sum of the strains  $\epsilon_H$  and  $\epsilon_T$  from hydrostatic and triaxial loading respectively.  $\epsilon_H$  is just the linear compression due to a hydrostatic pressure equal to  $\sigma_3$ . We obtain  $\epsilon_T$  from a triaxial compression experiment at constant confining pressure equal to  $\sigma_3$  at that point on the stress-strain curve when the lateral strain, an extension, just equals the linear compression due to confining pressure  $\sigma_3$ . In other words, it is the point on the stress-strain curve where the lateral shortening due to confining pressure is just balanced by the lateral extension due to axial stress.

A second test of path dependence is given by comparison of stresses in the  $\sigma_1$  direction. Our question here is, does the total axial stress in a triaxial experiment equal  $\sigma_1$  in the uniaxial strain experiment, when total lateral strain is zero in both?

Triaxial experiments in which both axial and radial strains were measured were available from a previous study of dilatancy [30] for Westerly granite and marble. Although Solenhofen limestone has been widely studied, complete strain data from triaxial experiments are unknown to us. Eight experiments were carried out to provide the required information, using jackets and strain gauges identical to those used in uniaxial loading as described above.

Comparison following the two schemes outlined above is shown in Fig. 7 for Westerly granite, Fig. 8 for marble, and Fig. 9 for Solenhofen limestone. In each, we show all or portions of the curves of  $\sigma_1$  vs  $\sigma_3$  and  $\sigma_1$  vs  $\epsilon_1$  given above and tabulated in Table 2, for comparison with points from triaxial experiments at which total lateral strain was zero.

Comparison of the uniaxial with the combined hydrostatic-triaxial data reveals very close agreement in the strains for granite and limestone except at high pressures, and a small (10 percent) but consistent difference for the marble. Comparison of the stresses for the three rocks (the left hand curve in each figure) gives agreement within about 5 percent for all three of the rocks, except granite at high pressure. For the marble, triaxial values are consistently below; for the granite, above; and for the limestone alternating above and below the values obtained in uniaxial loading.

Without further work it is not known whether the differences cited above reflect small but real differences due to path, or

whether they are experimental. Of the three, the most careful comparison was made in the case of Sclenhofen; for the other rocks, the samples used came from different blocks or from different orientations in the same block. This last factor may be particularly critical for the marble, which is elastically anisotropic [25] to a degree consistent with the differences noted above.

We conclude that path dependence in our three rocks is of the same order as the path dependence of the stress at faulting reported in [9]; that is, variations due to path are 10 percent or less. This result is of some interest owing to the wide range of mechanical properties of the three rocks. Under the conditions of the experiments, granite was brittle, and marble was ductile except near room pressure. The limestone was brittle at low pressure and ductile at high pressure if we adopt from HEARD [31] the mean stress (2.7 kb) at which he observed the brittle-ductile transition. In addition, pore collapse occurs at the higher stresses in the limestone. Apparently, then, relative insensitivity to loading path is a common feature of both stress-strain behavior (our result) and ultimate strength [9] of rocks.

#### Dilation and failure in relation to uniaxial deformation

The stress paths during uniaxial deformation are shown for all of the rocks in Fig. 1. Clearly stresses were non-hydrostatic even for the weakest rocks, and it is of interest

to determine why a particular rock followed a particular path. From consideration of recoverable behavior [18] and from examination of the curves in Fig. 1, the determining factors seem to be: intrinsic elastic properties, crack characteristics, and the tendency to fail locally by pore collapse or by intracrystalline flow. Of all the rocks, only the diabase followed a stress path (Fig. 1) which could have been predicted purely from elastic properties of the minerals [18]. Several of the other low porosity rocks, for example, the granites, the marble, and the gabbro were truly elastic only in regard to nondeviatoric strain; their curves in Fig. 1 reflect a combination of elastic strain and relaxation due to sliding on closed cracks. The relative importance of sliding on cracks may be found by comparison of rocks of similar mineralogy for which, therefore, elastic strains would be identical. Apparently motion on cracks played a greater role for gabbro than for diabase, and for Barre than for Westerly granite. Unfortunately no more quantitative explanation of these differences is possible.

Certain of the rocks were clearly weakened by high porosity; for example, Navajo compared with Nugget sandstone, and rhyolite compared with the granites. However, it is curious that the stress paths of the calcite rocks (marble, Bedford and Solenhofen limestones) do not reflect differences in porosity, particularly at high stress levels. Perhaps the low shear strength of calcite dominated here.

Rocks typically increase in volume nonelastically during triaxial compression (termed dilatancy or dilation) at a stress difference which is about half to two thirds the fracture length [30, 29]. Where does dilation begin relative to the point in a triaxial experiment at which strain is uniaxial? The stress at which dilation is first detected, the dilation stress, was previously determined for two of the rocks studied here, Westerly granite and marble. In Fig. 7 the dilation stress (heavy bar) is compared for a number of experiments at different confining pressure,  $\sigma_3$ , with the value of  $\sigma_1$  (open x) at which total lateral strain in the triaxial experiments is zero. As discussed in the last section, we also give in Fig. 7 the curve (dotted) obtained in the present study by uniaxial loading. Comparison of the three sets of data shows fair agreement except at  $\sigma_3 = 0$ . The dotted curve, representing the stresses at uniaxial strain obtained here, appears to be within about 10 percent of the dilation stress.

A similar comparison for marble is given in Fig. 8 with uniaxial data from the same source. For this rock dilation was only observed below  $\sigma_3$  of about 4 kb [32, 29]. The dilation stress (solid bar) is very close to the uniaxial strain point (square) from the triaxial experiment; it is systematically below the curve through the values measured here.

The dilation stress is known for another granite from the work of MATSUSHIMA [33]. This rock, the Kitashirakawa granite,

has a grain size two to three times that of Westerly granite, but has quite similar mineralogy, containing 80 percent feldspar, 10 percent quartz, and 8 percent biotite. The dilation and fracture stresses are compared with those of Westerly granite in Fig. 10; the dilation stresses for these rocks are quite similar, although Westerly is about 25 percent stronger than the Kitashirakawa granite.

#### Implications for failure theory of rocks

In previous studies, PAULDING [34] and BRACE and BYERLEE [35] tested the applicability of Griffith theory of fracture, modified to include friction on closed cracks, to brittle fracture of rocks under pressure. Both from theoretical considerations and from observation of the way elastic properties changed as stress increased to fracture, it seemed more likely that Griffith theory predicts the dilation stress rather than the stress at which fracture by faulting occurs. However, in the light of present results, even this modified view may have to be rejected. For one thing, the dilation stress does not appear to be very structure-sensitive, as was shown by comparison of data for the two granites (Fig. 10). For Griffith theory to apply, dilation stress should vary with initial crack length, which is, presumably, closely related to grain size. For another thing, agreement of the dilation stress with the point of zero lateral strain for three very different rocks suggests that the dilation stress may be controlled more by geometrical than by microstructural or mineralogic factors.

Much more work is needed here for a fuller understanding of the dilation stress, and a particularly interesting area of study is behavior under more general stress states. Experiments with three unlike compressions will provide an important test of the consistency of our observations.

The results near atmospheric pressure (Figs. 7, 10) raise a number of questions. The dilation stress, from the previous measurements, is of the order of half the fracture stress, which is obviously different from the point of uniaxial strain. For an experiment at  $\sigma_3 = 0$ , strain is uniaxial only at  $\sigma_1 = 0$ . Clearly the situation at room pressure is different, then, from that in a confined compression test at a pressure above a few hundred bars. Does this mean, on the one hand, that the detailed fracture process is different in the two cases? There seems to be some evidence for this in recent crack studies [36, 37]. Or does it mean, on the other hand, that the dilation stress has been incorrectly measured in experiments at low pressure? Does dilation actually begin close to zero stress, as suggested by the present correlation? Clearly these questions need to be resolved.

Acknowledgments - This research was supported by Advanced Research Projects Agency (ARPA) and the Defense Atomic Support Agency (DASA) and was monitored by DASA under Contract No. DASA 01-69-C-0122. Discussion with Clifton McFarland, J.B. Walsh, and S.P. Green was particularly helpful. Prof. S. Matsushima of Kyoto University assisted by providing a thin section of the Kitashirakawa granite.

## REFERENCES

1. JONES, A.H., and FROULA, N.H. Uniaxial strain behavior of four geological materials to 50 kilobars. DASA-2209 (1969).
2. BUTKOVICH, T.R. Calculation of the shock waves from an underground nuclear explosion in granite. J. Geophys. Res. 70, 885-892 (1965).
3. HUBBERT, M. KING, and WILLIS, David G. Mechanics of hydraulic fracturing. Am. Inst. Min. Metall. Engrs. Trans. 210, 153-166 (1957).
4. SERATA, Shosei. Transition from elastic to plastic states of rocks under triaxial compression. 4th Symposium on Rock Mechanics, Bull. of Min. Indus. Exper. Station, Penn State Univ., 73-82 (1961).
5. HENDRON, A.J. The behavior of sand in one-dimensional compression. RTD-TDR-63-3089, AFWL, Kirtland Air Force Base, New Mexico (1963).
6. TZUNG, Fu-Kong. Sand in one-dimensional compression. Unpublished MS Thesis, University of Utah (June, 1966).
7. BROWN, W.S., DE VRIES, K.L., and SMITH, J.L. Properties of rocks tested in one-dimensional compression. Tech. Rept. No. AFWL-TR-66-124, Univ. of Utah (January, 1967).

SMITH, J.L., DE VRIES, K.L., BUSHNELL, D.J., and BROWN, W.S. Fracture data and stress-strain behavior of rocks in triaxial compression. Experimental Mechanics 9, 348-355 (1969).

BROWN, W.S., and SWANSON, S.R. Constitutive equations for Westerly granite and Cedar City tonalite for a variety of loading conditions. Final Rept. DASA-2473, 120 pp. (1970).

MCQUEEN, R.G., MARSH, S.P., and FRITZ, J.N. Hugoniot equation of state of twelve rocks. J. Geophys. Res. 72(20), 4999-5036 (1967).

LOMBARD, D.B. The Hugoniot equation of state of rocks. LRL-UCRL-6311, G-3294, Univ. of Calif. (1961).

AHRENS, T.J., and GREGSON, V.G., Jr. Shock compression of crustal rocks; data for quartz calcite and plagioclase rocks. J. Geophys. Res. 69(22), 4839-4874 (1964).

PETERSEN, C.R., MURRI, W.J., and COWPERTHWAITTE, M. Hugoniot and release-adiabat measurements for selected geologic materials. J. Geophys. Res. 75(11), 2063-2072 (1970).

AHRENS, T.J., and ROSENBERG, J.N. "Shock metamorphism; experiments on quartz and plagioclase", in Shock Metamorphism of Natural Materials (B.M. French and N.M. Short, Eds.), Mono Book Corp., Baltimore (1968).

15. GIARDINI, A.A., LAKNER, J.F., STEPHENS, D.R., and STROMBERG, H.D. Triaxial compression data on nuclear explosion shocked, mechanically shocked, and normal granodiorite from the Nevada Test Site. J. Geophys. Res. 73(4), 1305-1320 (1968).
16. GREGSON, V.G., Jr., ISBELL, W.M., and GREEN, S.J. Yield of Westerly granite under shock loading. Trans. Amer. Geophys. Union 51(4), 423 (1970).
17. BRACE, W.F., and JONES, A.H. Comparison of uniaxial deformation in shock and static loading of three rocks. J. Geophys. Res., in press (1971).
18. WALSH, J.B., and BRACE, W.F. Elasticity of rock in uniaxial strain. Int. J. Rk. Mech. Min. Sci., in press (1971).
19. BRACE, W.F., and ORANGE, A.S. Further studies of the effects of pressure on electrical resistivity of rocks. J. Geophys. Res. 73(16), 5407-5420 (1968).
20. NUR, A., and SIMMONS, Gene. The effect of viscosity of a fluid phase on velocity in low porosity rocks. Earth & Plan. Sci. Letters 7, 99-108 (1969).
21. BRACE, W.F., ORANGE, A.S., and MADDEN, T.M. The effect of pressure on the electrical resistivity of water-saturated crystalline rocks. J. Geophys. Res. 70, 5669-5678 (1965).

2. PERKINS, R.D., GREEN, S.J., and FRIEDMAN, M. Uniaxial stress behavior of porphyritic tonalite at strain rates to  $10^3$ /second. Int. J. Rock Mech. Min. Sci. 7, 527-535 (1970).
3. GREEN, S.J., and PERKINS, R.D. Uniaxial compression tests at strain rates from  $10^{-4}$ /sec to  $10^4$ /sec on three geologic materials. DASA-2199, Final Report, 44 pp. (1969).
4. WALSH, J.B., BRACE, W.F., and WAWERSIK, W.R. Attenuation of stress waves in Cedar City diorite. Tech. Rept. No. AFWL-TR-70-8, 76 pp. (1970).
5. BRACE, W.F. Some new measurements of linear compressibility of rocks. J. Geophys. Res. 70, 391-398 (1965).
6. BRACE, W.F. Effect of pressure on electric-resistance strain gages. Experimental Mechanics 4(7), 212-216 (1964).
7. PATERSON, M.S. Secondary changes of length with pressure in experimentally deformed rocks. Proc. Roy. Soc. London, A, 271, 57-87 (1963).
8. GRINE, D.R. Progress Letter No. 7, SRI Project PGU 7852, Stanford Research Inst., Menlo Park, Calif. (1970).
9. EDMOND, J.M. Effects of pressure during rock deformation, PhD thesis, Australian National University (1969).
10. BRACE, W.F., PAULDING, B.W., Jr., and SCHOLZ, C. Dilatancy in the fracture of crystalline rocks. J. Geophys. Res. 71(16), 3939-3953 (1966).

31. HEARD, H.C. "Transition from brittle fracture to ductile flow in Solenhofen limestone as a function of temperature, confining pressure, and interstitial fluid pressure", in Rock Deformation (D. Griggs and J. Handin, Eds.), GSA Memoir 79, Chap. 7, 193-226 (1960).
32. SCHOLZ, C.H. Microfracturing and inelastic deformation of rock in compression. J. Geophys. Res. 73, 1417-1432 (1968).
33. MATSUSHIMA, S. On the deformation and fracture of granite under high confining pressure. Disaster Prevention Res. Inst. Bull. No. 36, Kyoto Univ. (1960).
34. PAULDING, B.W., Jr. Crack growth during brittle fracture in compression. PhD. thesis, M.I.T. (1965).
35. BRACE, W.F., and BYERLEE, J.D. "Recent experimental studies of brittle fracture of rocks", in Failure and Breakage of Rock, Amer. Inst. of Mining, New York (1966).
36. WAWERSIK, W., and BRACE, W.F. Post-failure behavior in granite and diabase. J. of Internat. Soc. of Rock Mech., in press.
37. KOIDE, H. and HOSHINO, K. Development of microfractures in experimentally deformed rocks. Chi-sin (Earthquake) 20(2), 85-97 (1967).
38. BYERLEE, J.D. Frictional characteristics of granite under high confining pressure. J. Geophys. Res. 72(14), 3639-3648 (1967).

## CAPTIONS

- 1 Stress-strain relations during uniaxial loading. Along the line marked HYDROSTATIC,  $\sigma_1$  equals  $\sigma_3$ .
- 2 Stress in the axial direction as a function of axial strain. Curves are identified by abbreviated rock name. The small number on some of the curves is porosity in percent. The dotted lines are stress-strain curves which would be followed if porosity were zero.
- 3 Photomicrographs of Bedford limestone (a) before deformation and (b) after one cycle of loading in uniaxial strain along the path shown in Fig. 1.
- 4 Uniaxial strain behavior of Westerly granite. The open circles and triangles are static experiments, the closed squares for shock loading. GRINE's data pertain to Bradford granite.
- 5 Comparison of permanent volumetric compaction with initial porosity for high porosity rocks. Rock names are abbreviated. Size of boxes indicates uncertainty.
- 6 Comparison of axial strains in uniaxial loading (a) and in hydrostatic plus triaxial loading (b). The end state in each case is the same. The dotted figure in (b) is the position after hydrostatic loading, the dot-and-dash figure; the position after triaxial plus hydrostatic loading.

- Fig. 7 Dilation stress and uniaxial deformation compared for Westerly granite. The dotted curve of  $\sigma_1$  vs  $\sigma_3$  is from Fig. 4. The dotted area in the plot of  $\sigma_1$  vs  $\epsilon_1$  includes all of the data points for the granite, from Fig. 4. The boxes are points in triaxial experiments in which total lateral strain was zero from [30]. The bars give the approximate values of the dilation stress, also from [30].
- Fig. 8 Dilation stress and uniaxial deformation compared for marble. Symbols same as Fig. 7.
- Fig. 9 Path dependence of uniaxial deformation for Solenhofen limestone. Symbols same as Fig. 7.
- Fig. 10 Stress at fracture and dilation compared for Westerly and Kitashirakawa granites. The dotted band includes the values of stress at dilation from Fig. 7. Fracture stresses for Westerly are from [30, 38].

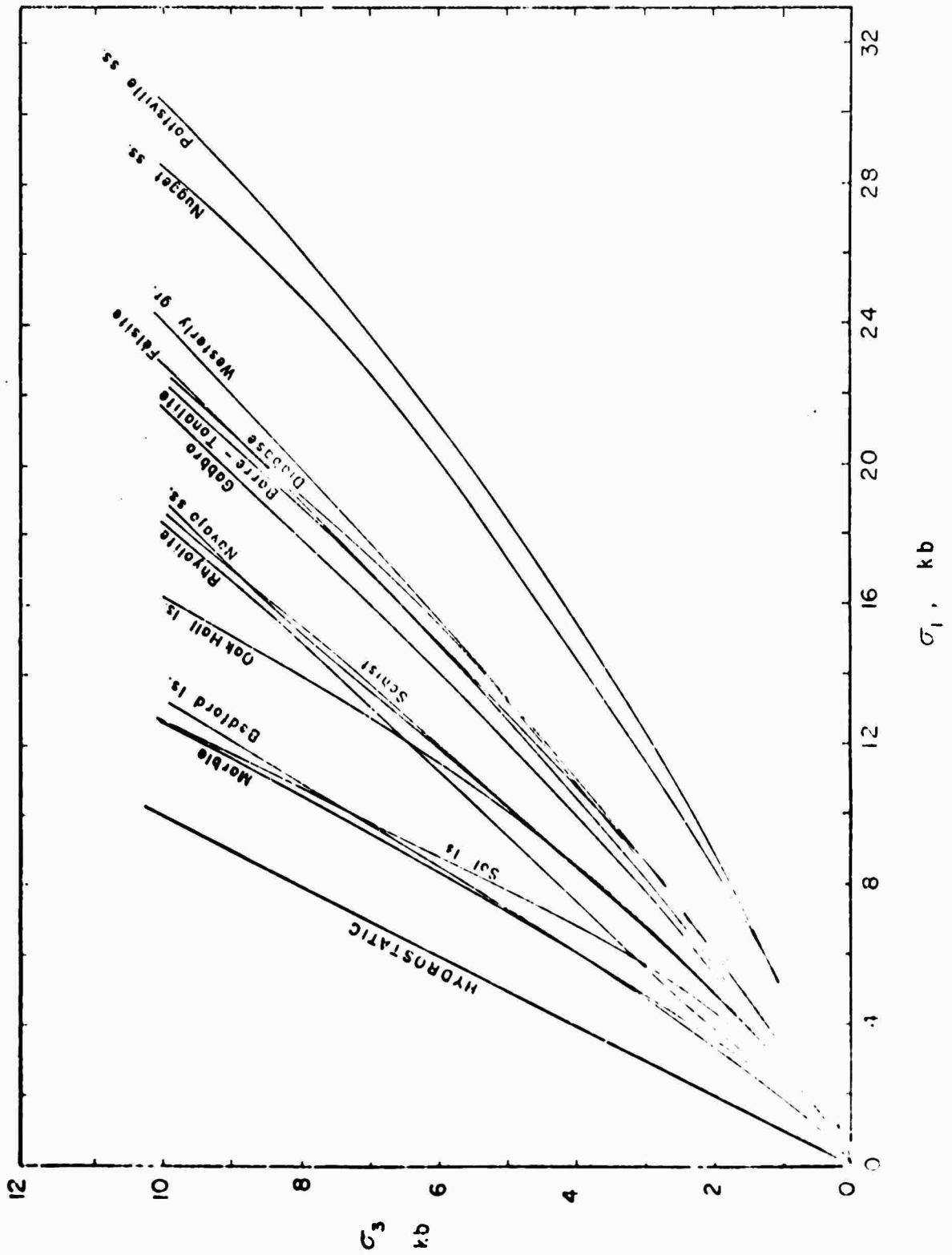


Fig. 1 Stress-strain relations during uniaxial loading

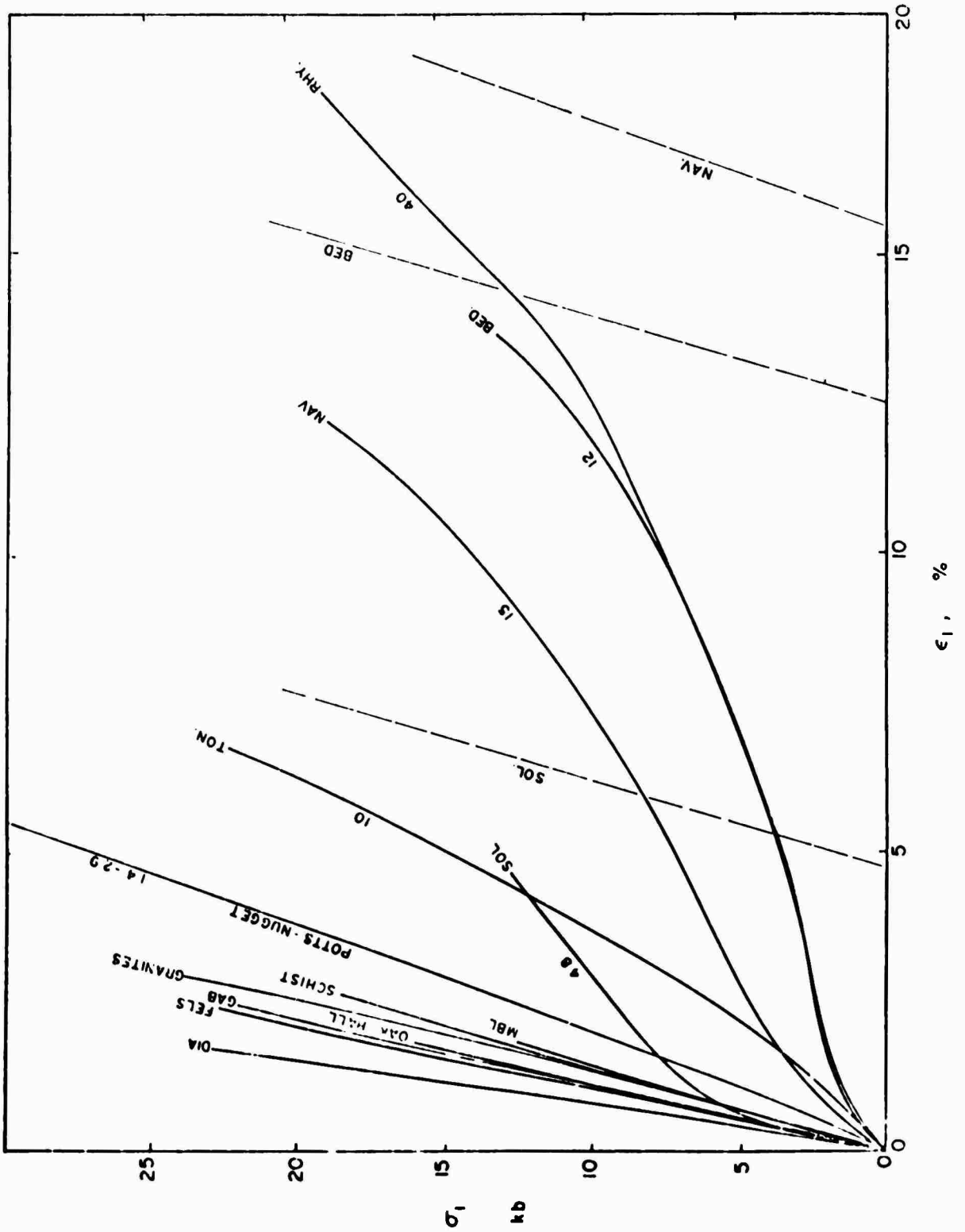
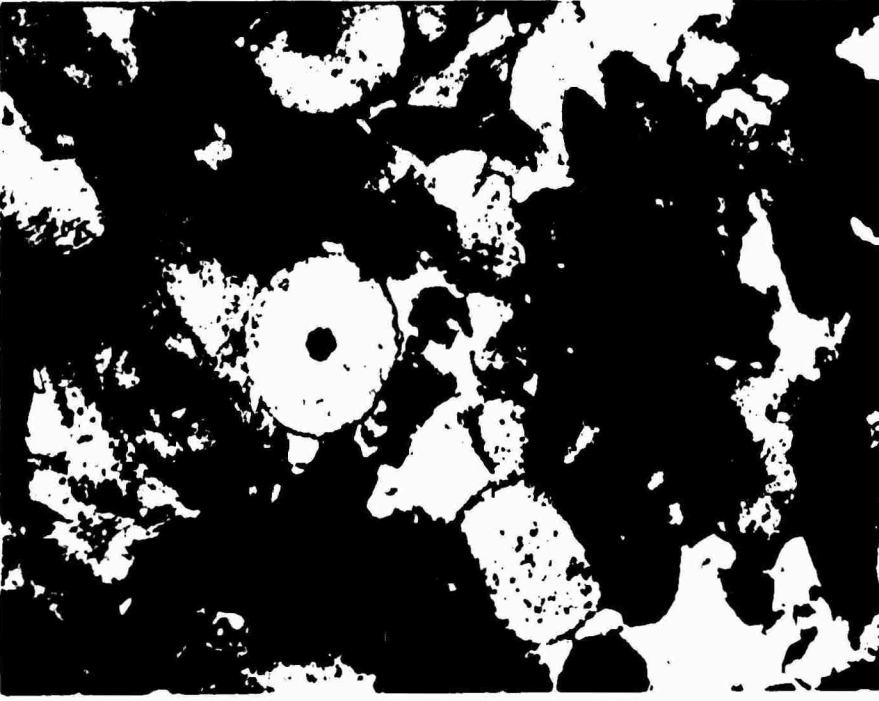


Fig. 2 Stress in the axial direction as a function of axial strain



(a)



(b)

Fig. 3 Photomicrographs of Bedford limestone (a) before deformation and (b) after one cycle of loading

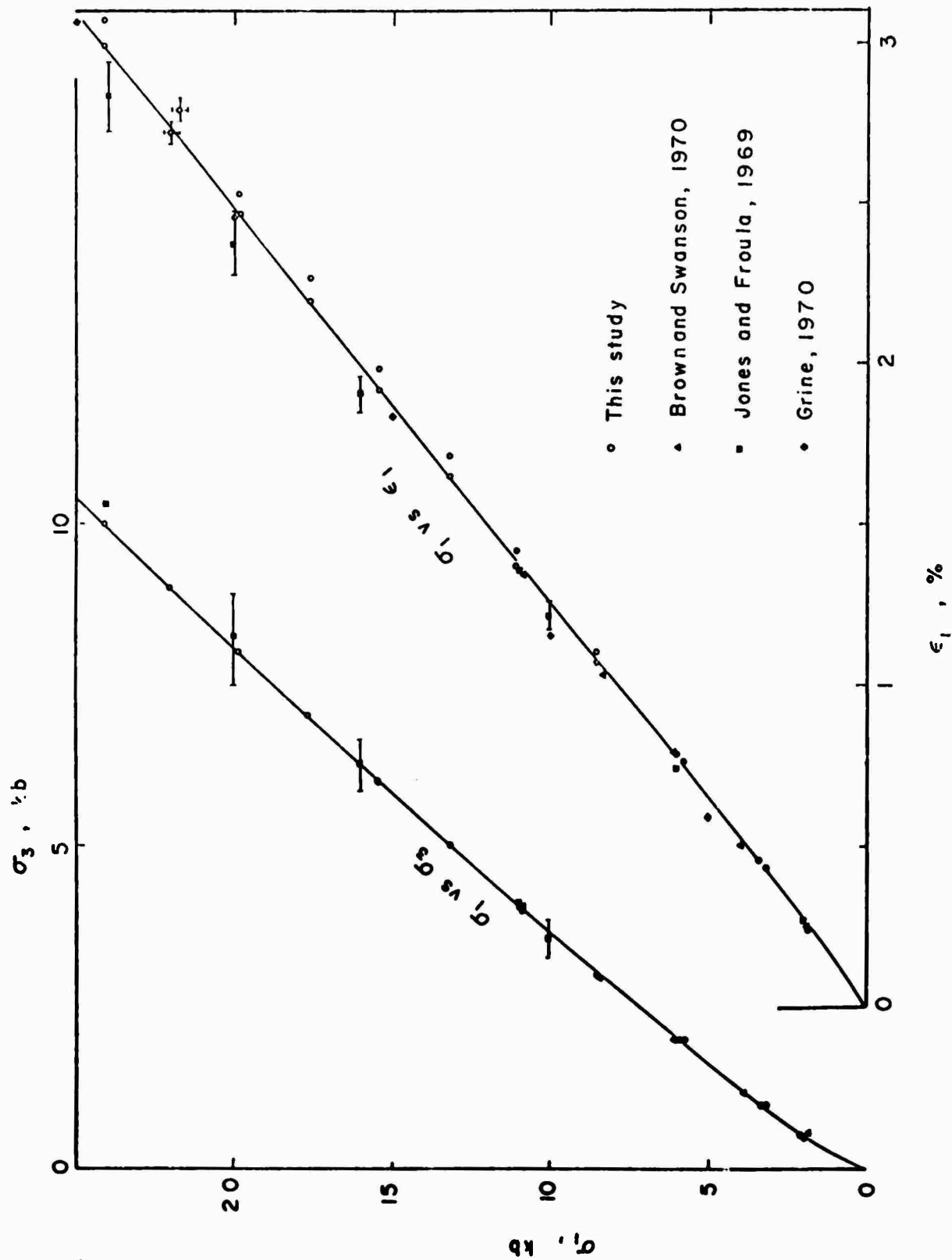


Fig. 4 Uniaxial strain behavior of Westerly granite

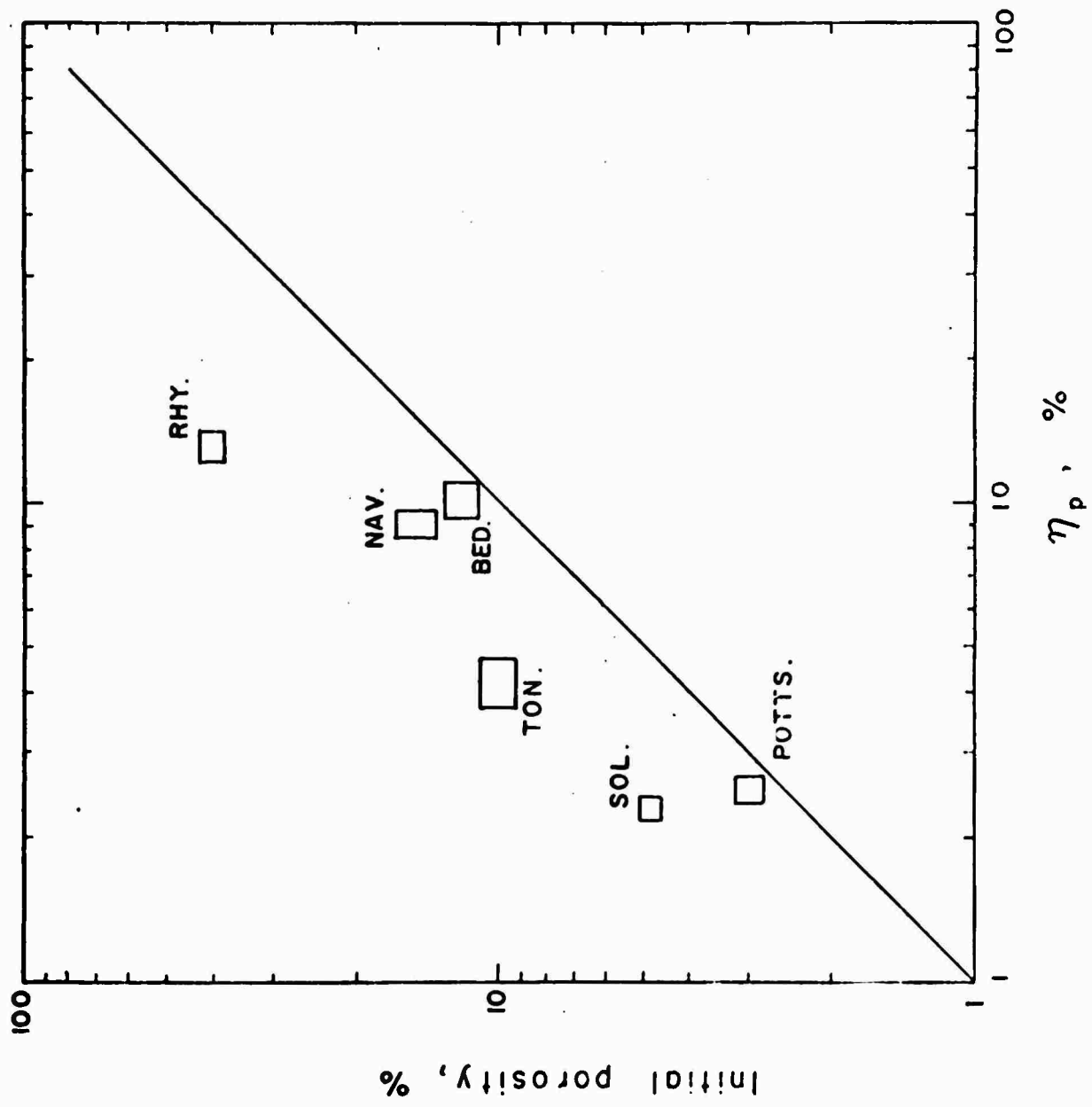


Fig. 5 Comparison of permanent volumetric compaction with initial porosity

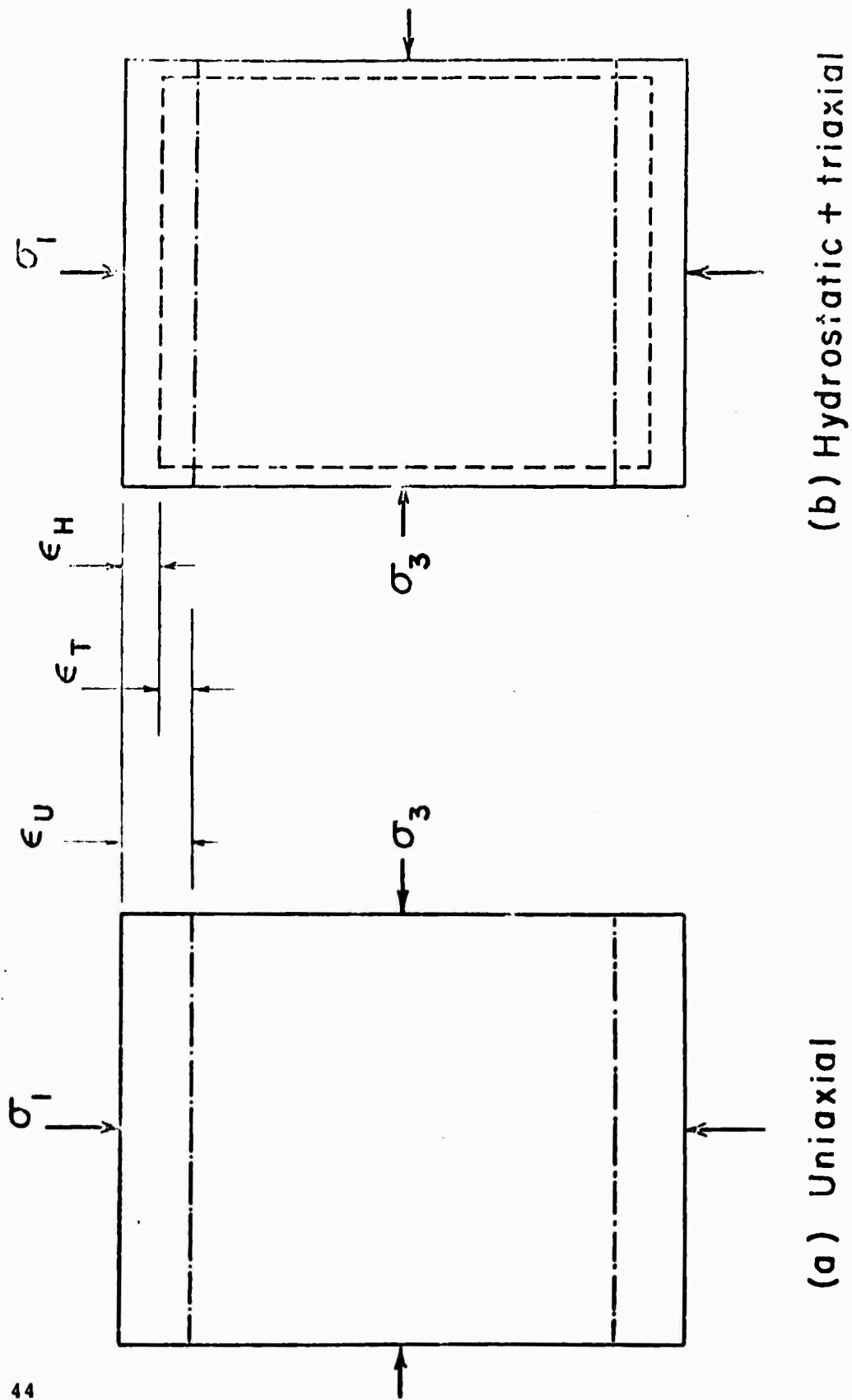


Fig. 6 Comparison of axial strains in uniaxial loading (a) and in hydrostatic plus triaxial loading (b)

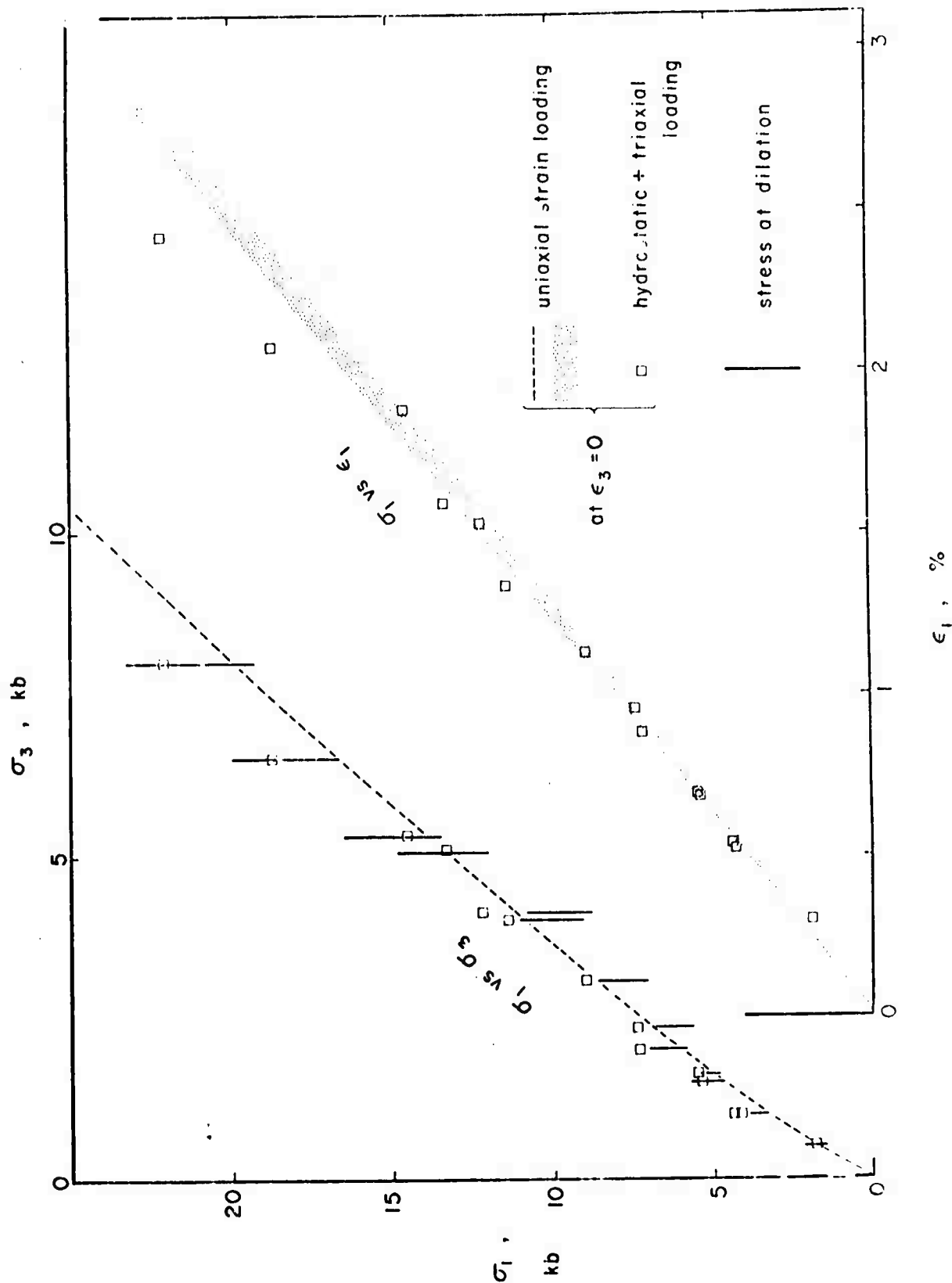


Fig. 7 Dilation stress and uniaxial deformation compared for Westerly granite

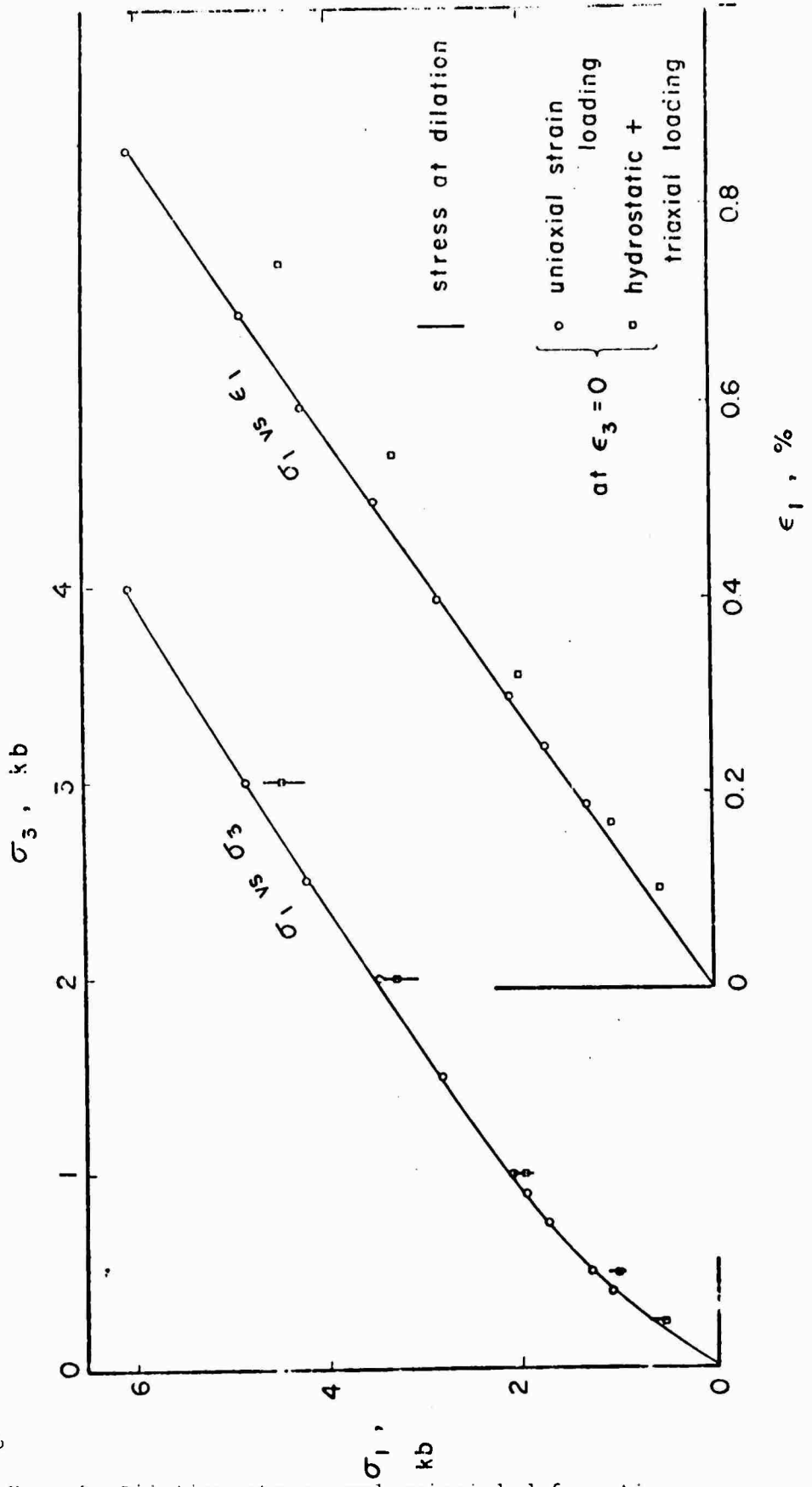


Fig. 8 Dilation stress and uniaxial deformation compared with marble

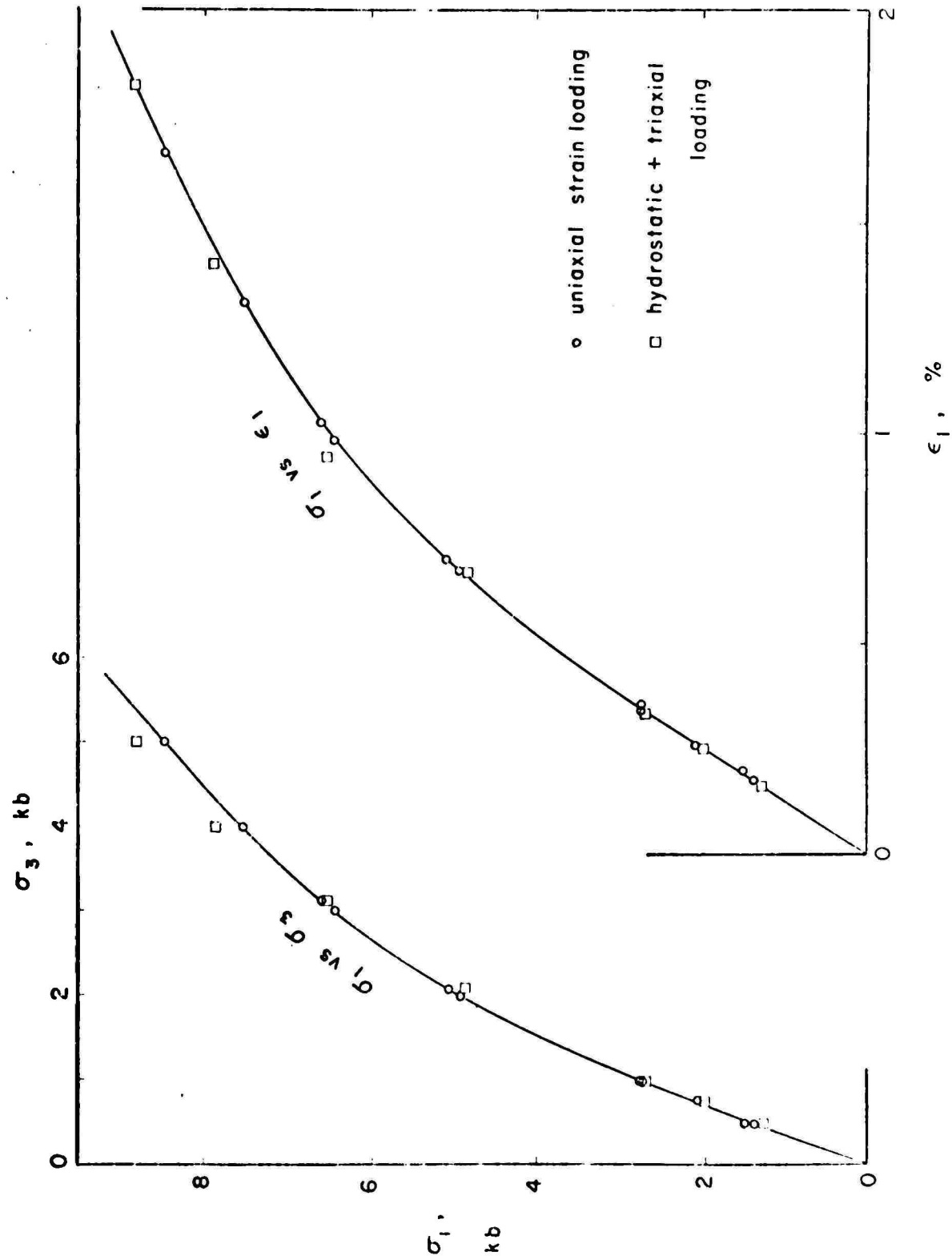


Fig. 9 Path dependence of uniaxial deformation for Solenhofen limestone

**END**